Available online at www.sciencedirect.com
ScienceDirect
Proceedings of the Combustion Institute xxx (2009) xxx–xxx
Proceedings of the Combustion Institute
www.elsevier.com/locate/proci

An assessment of gas-phase reaction mechanisms and soot models for laminar atmospheric-pressure ethylene–air flames

R.S. Mehta *, D.C. Haworth, M.F. Modest

Department of Mechanical and Nuclear Engineering, The Pennsylvania State University, 301 B Reber Building, University Park, PA-16802, USA

Abstract

A comprehensive assessment of gas-phase reaction mechanisms and soot models has been performed for atmospheric-pressure laminar ethylene–air flames. Soot modeling is based on a method of moments with interpolative closure. Computed soot volume fractions are compared with experimental measurements for eight flames: four premixed flames from two different burners, and four opposed-flow diffusion flames from two different burners. Seven gas-phase reaction mechanisms have been explored with variations in four key soot model parameters: PAH-based versus acetylene-based nucleation; PAH condensation included versus excluded; surface reactivity steric factor specification; and surface radicals depleted versus conserved. Computed soot volume fractions are most sensitive to variations in the surface reactivity factor and to whether the surface radicals are depleted or conserved. The motivation for this study has been to determine which models should be used for simulations of luminous turbulent flames; there computational efficiency is of paramount importance. A reduced 33-species mechanism together with acetylene-based nucleation, surface reactivity factor variation proposed by [J. Appel, H. Bockhorn, M. Frenklach, *Combust. Flame* 121 (2000) 122–136], and conserved surface radicals yields acceptable soot volume fractions over a broad range of conditions with an order of magnitude reduction in computational cost compared to a larger 100-species gas-phase reaction mechanism.

Keywords: Soot; Laminar flames; Method of moments

1. Introduction

Quantitative prediction of soot formation has been a long-standing challenge in combustion research, even in laminar flames [1]. Most combustion devices operate in a turbulent flow regime where turbulence–chemistry interactions (TCI) and turbulence–radiation interactions (TRI) influence mean soot levels [2–4]. To make progress in soot modeling for luminous turbulent flames, reaction mechanisms should be established and validated systematically in configurations where the confounding effects of TCI and TRI are absent.

To this end, a comprehensive modeling study of soot formation in laminar flames has been performed. The scope is limited to atmospheric-pressure ethylene–air flames and to soot modeling based on a method of moments [5]. Both premixed flames and opposed-flow diffusion flames are

* Corresponding author. Fax: +1 256 726 4806.
E-mail address: rsm@cfdrc.com (R.S. Mehta).

1540-7489/$ - see front matter © 2009 The Combustion Institute. Published by Elsevier Inc. All rights reserved.
doi:10.1016/j.proci.2008.06.149

considered with variations in gas-phase kinetics mechanisms and soot model parameters.

Principal contributions of this work are: (i) to systematically evaluate parameters in soot submodels combined with different gas-phase mechanisms available in the literature; (ii) to identify key sensitivities in these models; and (iii) to provide recommendations for soot modeling in turbulent flames.

2. Physical models and numerical methods

2.1. Gas-phase mechanisms

Seven gas-phase mechanisms have been evaluated (Table 1). The 100-species ethylene mechanism (ABF100) proposed by Appel, Bockhorn and Frenklach [6] is modified from the 99-species mechanism (WF99) proposed by Wang and Frenklach [7]; both of these include species up to four-ring polycyclic aromatic hydrocarbons (PAHs). Qin et al. [8] proposed a 70-species mechanism (QLY70) that includes species up to benzene. The QLY70 mechanism was reduced by Law [9] to a 33-species mechanism (QLY33) using the directed-relational-graph (DRG) method. MECHMOD [10] was used to reduce ABF100 to a 31-species mechanism (ABF31) that contains all the species common to ABF100 and QLY33. Williams and co-workers [11] developed an ethylene mechanism that contains 46 species (WI46). Li, Varatharajan and Williams [12] proposed a 19-species mechanism (LVW19) that contains 36 one-way reactions. All of these mechanisms contain only elementary reactions with no algebraic constraints. The authors are not aware of previous application of QLY70, WI46, ABF31 or LVW19 to soot modeling.

2.2. Soot models

Detailed and semi-detailed soot models generally have two parts: (i) soot kinetics (interaction between soot particles and the surrounding gas-phase species) that includes nucleation, surface growth and oxidation models; and (ii) soot-particle dynamics (interaction between the soot particles) that includes coagulation and aggregation. The soot particle dynamics can be treated in different ways. These include the method of moments where one solves for the moments of the particle-size distribution function (PSDF) [5], or sectional methods [13] where the PSDF is divided into discrete sections by average particle size. Here a method of moments with interpolative closure has been used. Three to six moments have been found to be sufficient in previous modeling studies of laminar premixed flames [6,14] and opposed-flow diffusion flames [15]. The method of moments can be extended to aggregation of soot particles into mass fractals [16]. Since the current study is limited to atmospheric-pressure flames, it is expected that soot particles will remain primarily spheroidal; hence aggregation is not considered.

Table 1
Gas-phase reaction mechanisms

Name	No. of species	No. of reactions	Ref. remark
WF99	99	533	[7]
ABF100	100	542	[6]
QLY70	70	463	[8]
QLY33	33	205	[8] Reduced by DRG [9]
WI46	46	235	[11]
ABF31	31	179	Retain species common to ABF100 and QLY33
LVW19	19	36	[12]

Two different nucleation mechanisms have been evaluated. Frenklach and co-workers proposed PAH-based nucleation mechanisms [14], while Lindstedt and co-workers used an approach based on acetylene concentration [3,17]. The authors are not aware of previous applications of the acetylene-based nucleation model to premixed flames. PAH-based nucleation mechanisms inherently require use of large gas-phase reaction mechanisms. Here soot coagulation is considered in free-molecular, continuum and transition regimes.

Soot surface growth models have been an active area of research for several decades [1]. Frenklach and Wang [14,18] proposed chemical similarity, which postulates that chemical reactions taking place on the soot particle surface are analogous to those for large PAH molecules [18]. The surface-HACA mechanism is consistent with the findings of Harris and Weiner [19], who identified that acetylene dominates surface growth in their flames. Soot surface oxidation is via attack by OH radicals and oxygen [20]. Here, the surface-HACA mechanism has been used [14]. A key element of that mechanism is that surface radicals are completely depleted during the acetylene addition step. Wang et al. [15] reported that this mechanism underpredicts soot by an order of magnitude in opposed-flow diffusion flames. They reported improved agreement with experiments with surface radicals conserved during the acetylene addition step. They also noted that reality probably lies somewhere between the two extremes of complete depletion and complete conservation of radical surface sites. The two extremes are considered here.

The surface reaction rate due to gaseous species (growth or oxidation) for a soot moment r can be written as,

$$W_r^{\mathrm{surf}} = k_{\mathrm{sg}} C_{\mathrm{g}} \alpha \chi_{\mathrm{s}} M_0 \sum_{k=0}^{r-1} \binom{r}{k} \Delta m^{r-k} \mu_{r+2/3} \qquad (1)$$

Please cite this article in press as: R.S. Mehta et al., *Proc. Combust. Inst.* (2009), doi:10.1016/j.proci.2008.06.149

where k_{sg} is the kinetic rate coefficient for reaction with gas g, C_g is the molar concentration of the gas species, α is a steric factor, χ_s is the nominal number density of surface radical sites, Δm is the change in soot mass due to the reaction [14] and μ_p is the reduced soot moment. The factor α is the fraction of the surface sites available for chemical reactions; it was introduced by Frenklach and Wang [18] to account for differences in soot surface growth rates with temperature as a result of structural changes. The functional form for α has evolved from constant values [14,21] to a temperature-dependent expression used by Appel, Bockhorn and Frenklach [6]. Here two different values of α are considered: $\alpha = 1$ (all the soot surface sites are available for reaction) and $\alpha = \alpha_{ABF00}$, corresponding to the functional form introduced by Appel, Bockhorn and Frenklach [6]. The latter includes a dependence on soot particle size as well as temperature. The authors are not aware of previous application of α_{ABF00} to laminar opposed-flow diffusion flames. The importance of PAH condensation on soot surface growth also has been a much-researched topic [22], and a model for that process is included in the method of moments whenever PAH molecules are present in the gas-phase mechanism.

2.3. Numerical tools

The laminar flames have been simulated using PREMIX [23] and OPPDIF [24]. Species scrubbing due to reactions with soot is included. Both codes have been modified to handle soot moments [6,15] as additional scalars. The molecular transport properties and gas-phase kinetics have been implemented using TRANSPORT [25] and CHEMKIN-II [26], respectively. Mixture-averaged diffusion properties are used for the gas-phase species. Differential and thermophoretic diffusion are included for soot moments as in [6,15]. The thermodiffusion of gas-phase species was neglected. The soot moments are modeled based on the average number of carbon atoms present per unit volume. This implies that the higher moments attain very large values. Hence, scaling is necessary to obtain stable numerical solutions. Here transport equations are solved for the natural logarithms of the soot moments. Achieving convergence with PREMIX was relatively straightforward. OPPDIF was more problematic. There numerical convergence was obtained by gradually ramping up the soot moment source terms over time until a converged steady-state solution was obtained.

3. Flame configurations

Eight flames are included in the present study (Table 2).

Table 2
Laminar flames modeled

Name	Type	Ref.	Remark
XSF97_1	Premixed	[27]	C/O = 0.78
XSF97_2	Premixed	[27]	C/O = 0.88
XSF97_3	Premixed	[27]	C/O = 0.98
ZYW03_1	Premixed	[28]	C/O = 0.69
WDS96_1	Diffusion	[15]	$a = 117$/s
WDS96_2	Diffusion	[15]	$a = 79$/s
HC01_1	Diffusion	[30]	
HC01_2	Diffusion	[30]	

3.1. Laminar premixed flames

Steady, one-dimensional, burner-stabilized ethylene/air flames have been modeled. In all cases, the measured temperature profiles have been prescribed in PREMIX. Xu, Sunderland and Faeth [27] measured temperature, species and soot volume fractions for different C/O ratios (equivalence ratios). These flames were studied by Appel, Bockhorn and Frenklach [6]. Here three of these flames have been modeled. For a similar configuration, Zhao et al. [28] reported PSDF, soot volume fraction and temperature profiles. This flame was simulated by Singh et al. [29] using a different soot-particle dynamics model.

3.2. Laminar diffusion flames

In contrast to premixed flames, diffusion flames have strongly oxidizing regions, thereby emphasizing different physics in the models. Wang et al. [15] studied four opposed-flow ethylene flames with different strain rates, a, and reported velocity and soot-volume-fraction profiles. They modeled the flames using a method of moments, with surface HACA for soot growth. They also explored sensitivity of computed temperature profiles to thermal radiation (using an optically thin model) and found that temperatures dropped by less than 1 K over the entire domain. Here, two of these flames are modeled including solving the energy (T) equation, with no radiation correction. In another study, Hwang and Chung [30] studied opposed-flow diffusion flames, including oxygen-enriched flames. They proposed different rate coefficients for the surface HACA mechanism. Two of their flames (those having oxygen concentrations similar to standard air) are simulated in the current study.

4. Results and discussion

4.1. Gas-phase species

Acetylene is a key species in soot models. Computed and measured C_2H_2 profiles for the XSF97_2 flame are shown in Fig. 1. Significant

Please cite this article in press as: R.S. Mehta et al., *Proc. Combust. Inst.* (2009), doi:10.1016/j.proci.2008.06.149

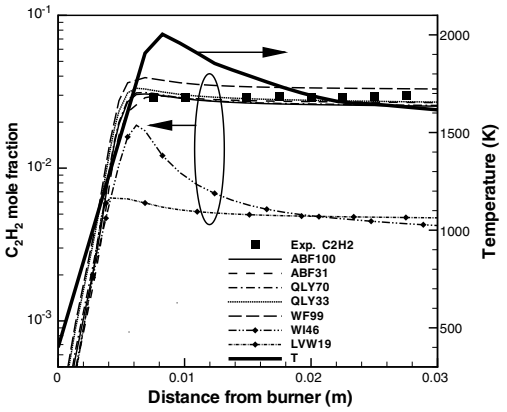

Fig. 1. Computed and measured C_2H_2 mole fraction profiles for the XSF97_2 premixed flame. The temperature profile is also shown.

underprediction of C_2H_2 and soot were found in all flames for WI46 and LVW19 regardless of the nucleation and surface growth parameters. Based on this, the WI46 and LVW19 mechanisms were removed from further consideration.

The combinations of gas-phase mechanisms and soot submodels for nucleation, PAH condensation and surface growth parameters for the remaining comparisons are shown in Table 3. For example, the only difference between Model 1 and Model 17 is that PAH condensation is considered in Model 1 and is neglected in Model 17. Similarly the difference between Model 17 and Model 18 is that surface radicals are depleted in Model 17 and are conserved in Model 18.

4.2. Laminar premixed flame structure

Computed flame structures for flames XSF97_1, XSF97_2 and XSF97_3 are similar to those reported in earlier studies [6]. Typical computed and measured species and soot volume fractions for several models are shown in Figs. 1 and 2. For the ZYW03_1 flame, measured profiles had to be shifted 3 mm upstream towards the burner to obtain a good match with experiments. This is consistent with the findings of Singh et al. [29]. Comparisons of individual terms in the soot moment equations reveal that the surface reaction rates are much more important than nucleation rates (not shown). This implies that the overall soot yield should be relatively insensitive to the nucleation submodel (PAH-based versus acetylene-based), and this is borne out in the results. The first six soot moments have been retained here. Computed soot volume fractions with three moments differ little from the six-moment results. Therefore, only three soot moments have been retained for the diffusion flame calculations.

4.3. Laminar diffusion flame structure

Following an approach similar to that reported in [15], boundary conditions were modified slightly to line up computed velocity profiles with experimental measurements. This should have negligible influence on the main mixing zone. Computed and measured velocity profiles for flames WDS96_1 and WDS96_2 are in good agreement (Fig. 3). Velocity profiles are not available for flames HC01_1 and HC01_2. However, the computed and measured stagnation point locations are in good agreement (not shown).

4.4. Soot volume fractions

Overall flame structures are well captured for both premixed and diffusion flames. To compare the performance of the many model variants, the principal figure-of-merit is taken to be the soot volume fraction at one point in the flame. For diffusion flames, this is simply the peak value. For premixed flames, it is the value at the last product-side data point reported in the experiments. Ratios of computed to measured soot volume fractions for 36 model variations are reported in Table 3. The ideal model would have values close to unity for all eight flames. To facilitate interpretation of Table 3, ratios greater than unity are in bold font, and ratios in the range 0.2 to 5.0 are shaded and bold. This choice of range is somewhat arbitrary, but serves to sort those models that do not perform well across a wide range of flames (rows with few or no shaded entries—e.g. Model 19) from those that are promising (rows with many shaded entries—e.g., Model 33). Space limitations preclude detailed discussion of all results. A few highlights are emphasized here.

Model 11 was proposed by Appel, Bockhorn and Frenklach [6] and applied to flames XSF97_1, XSF97_2 and XSF97_3. Soot volume fractions for XSF97_3 are under-predicted by Model 11, as reported in [6]. However, a variant that conserves surface radicals (Model 12) predicts the soot volume fraction well.

Examples of computed and measured soot volume fractions for a diffusion flame are provided in Fig. 4. Models 1 and 2 were used by Wang et al. [15], and their results are reproduced here. Models 9, 11, 13, 15 and 16 also are shown in Fig. 4.

Figure 5 compares results from a C_2H_2-based nucleation model (Model 16) with those from an otherwise identical model that uses PAH-based nucleation (Model 24) for a premixed flame and a diffusion flame. For the premixed flame (Fig. 5a), the predicted number density with C_2H_2-based nucleation is approximately a factor of two higher, and the soot volume fractions are also higher, although by a lesser factor. On the other hand, the soot volume fraction prediction in the diffusion flame is almost independent of

Please cite this article in press as: R.S. Mehta et al., *Proc. Combust. Inst.* (2009), doi:10.1016/j.proci.2008.06.149

Table 3
Ratios of computed to measured peak soot volume fractions for 36 models in eight flames (Table 2)

Model parameters						Ratio of computed to measured (peak) soot volume fractions							
						Diffusion flames				Premixed flames			
Model	Chemistry	Nucl. mech	PAH cond.	Surf. factor	Surface radicals	WDS96_1	WDS96_2	HC01_1	HC01_2	XSF97_1	XSF97_2	XSF97_3	ZYW03_1
1	WF99	PAH	Y	1.0	Dep	0.0036	0.0027	0.023	0.12	**0.99**	**1.7**	0.10	0.00034
2	WF99	PAH	Y	1.0	Con	**0.99**	**0.79**	**26**	**19**	**13**	**35**	**3.8**	0.0066
3	WF99	PAH	Y	ABF	Dep	0.00068	0.00056	0.0031	0.0056	0.075	0.13	0.10	0.00028
4	WF99	PAH	Y	ABF	Con	0.056	0.043	**0.25**	**0.67**	**0.58**	**1.5**	**0.46**	0.0026
5	WF99	C2H2	N	1.0	Dep	**1.3**	**0.70**	**1.5**	**2.3**	**11**	**5.0**	**0.24**	0.040
6	WF99	C2H2	N	1.0	Con	**46**	**27**	**30**	**19**	**16**	**6.6**	**5.5**	**1.6**
7	WF99	C2H2	N	ABF	Dep	0.11	0.062	0.082	0.041	1.5	**0.75**	0.069	0.025
8	WF99	C2H2	N	ABF	Con	**4.6**	**2.6**	**3.6**	**2.9**	**9.6**	**5.0**	**1.8**	**0.38**
9	ABF100	PAH	Y	1.0	Dep	**0.62**	**0.45**	**1.9**	**2.6**	**8.4**	**3.8**	**0.33**	0.017
10	ABF100	PAH	Y	1.0	Con	**65**	**41**	**77**	**27**	**97**	**54**	**11**	**0.24**
11	ABF100	PAH	Y	ABF	Dep	0.18	0.15	**0.66**	**0.90**	**0.62**	**0.33**	0.13	0.013
12	ABF100	PAH	Y	ABF	Con	**5.0**	**3.6**	**47**	**84**	**5.0**	**3.1**	**1.2**	0.081
13	ABF100	C2H2	N	1.0	Dep	**1.2**	**0.68**	**1.4**	**2.3**	**11**	**4.6**	**0.23**	0.033
14	ABF100	C2H2	N	1.0	Con	**45**	**24**	**30**	**19**	**16**	**5.8**	**5.2**	**1.1**
15	ABF100	C2H2	N	ABF	Dep	0.11	0.060	0.080	0.041	**1.7**	0.69	0.067	0.021
16	ABF100	C2H2	N	ABF	Con	**4.3**	**2.4**	**3.7**	**2.8**	**9.5**	**4.5**	**1.6**	**0.30**
17	WF99	PAH	N	1.0	Dep	0.0035	0.0026	0.021	0.11	**0.99**	**1.7**	0.09	0.00031
18	WF99	PAH	N	1.0	Con	**0.99**	**0.78**	**25**	**18**	**13**	**35**	**3.8**	0.0065
19	WF99	PAH	N	ABF	Dep	0.00060	0.00047	0.0022	0.0039	0.075	0.12	0.027	0.00025
20	WF99	PAH	N	ABF	Con	0.055	0.042	**0.24**	**0.64**	**0.58**	**1.5**	**0.45**	0.0025
21	ABF100	PAH	N	1.0	Dep	**0.45**	**0.29**	**0.95**	**1.6**	**8.3**	**3.7**	**0.25**	**0.30**
22	ABF100	PAH	N	1.0	Con	**60**	**36**	**48**	**5.8**	**96**	**54**	**11**	**0.23**
23	ABF100	PAH	N	ABF	Dep	0.092	0.069	**0.20**	**0.20**	**0.59**	**0.31**	0.087	0.010
24	ABF100	PAH	N	ABF	Con	**4.3**	**2.9**	**11**	**10**	**5.0**	**3.0**	**1.1**	0.076
25	QLY70	C2H2	N	1.0	Dep	**1.0**	**0.90**	**0.83**	**1.2**	**13**	**6.1**	**0.26**	0.12
26	QLY70	C2H2	N	1.0	Con	**44**	**29**	**23**	**13**	**17**	**7.8**	**5.8**	**5.0**
27	QLY70	C2H2	N	ABF	Dep	0.083	0.060	0.051	0.028	**2.0**	**0.9**	0.072	0.059
28	QLY70	C2H2	N	ABF	Con	**4.1**	**2.9**	**2.9**	**1.9**	**11**	**5.9**	**1.7**	**1.04**
29	QLY33	C2H2	N	1.0	Dep	**2.2**	**2.0**	**2.1**	**1.9**	**11**	**6.1**	**0.35**	**0.20**
30	QLY33	C2H2	N	1.0	Con	**57**	**36**	**34**	**11**	**16**	**6.6**	**5.4**	**7.9**
31	QLY33	C2H2	N	ABF	Dep	0.16	0.13	0.12	0.053	**2.1**	**0.99**	0.092	0.088
32	QLY33	C2H2	N	ABF	Con	**9.6**	**6.9**	**7.9**	**4.4**	**11**	**5.9**	**3.6**	**1.9**
33	ABF31	C2H2	N	1.0	Dep	**2.3**	**2.1**	**2.9**	**2.0**	**9.9**	**4.8**	**0.21**	**0.13**
34	ABF31	C2H2	N	1.0	Con	**54**	**36**	**35**	**16**	**13**	**6.2**	**4.5**	**3.8**
35	ABF31	C2H2	N	ABF	Dep	0.19	0.15	0.17	0.066	**1.6**	**0.75**	0.062	0.060
36	ABF31	C2H2	N	ABF	Con	**9.2**	**7.0**	**8.5**	**4.2**	**8.3**	**4.4**	**1.6**	**0.67**

Please cite this article in press as: R.S. Mehta et al., *Proc. Combust. Inst.* (2009), doi:10.1016/j.proci.2008.06.149

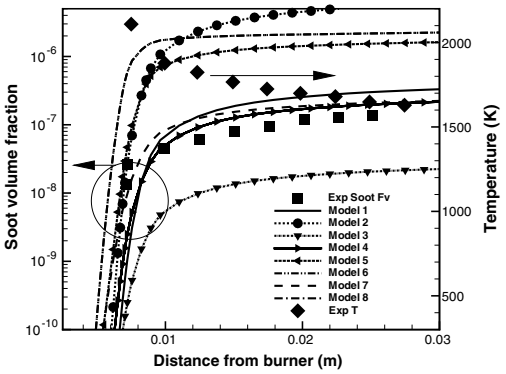

Fig. 2. Computed and measured soot volume fractions with different models for premixed flame XSF97_1.

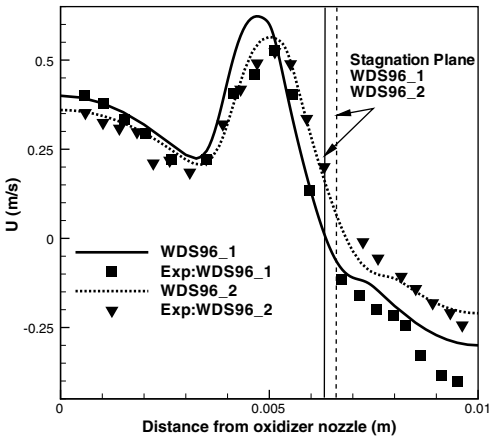

Fig. 3. Computed (lines) and measured (symbols) velocity profiles for WDS96_1 and WDS96_2 diffusion flames.

the nucleation mechanism, as observed by Leung, Lindstedt and Jones [17]. This implies that most of the soot production in opposed-flow diffusion flames results from surface reactions.

The effects of PAH condensation and surface reactions are shown in Fig. 6. The overall contribution of PAH condensation is relatively small compared to surface reactions for the diffusion flames. This is true even when surface radicals are depleted. The effects of PAH condensation for premixed flames are even smaller (Table 3).

Models 11 and 15 (surface radicals depleted) tend to underpredict soot by approximately one order of magnitude, while Models 12 and 16 (surface radicals conserved) overpredict soot in most flames by factors of four-to-five (Table 3). This suggests that something between complete depletion and full conservation might be appropriate. A function might be devised that depends on local conditions, similar to what has been done with the steric factor α [6].

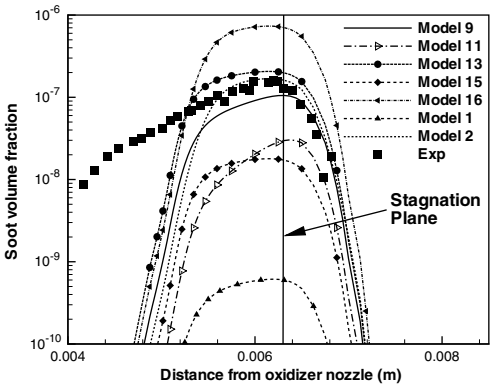

Fig. 4. Computed and measured soot volume fraction profiles with different models for WDS96_1 flame.

The influence of gas-phase reaction mechanisms on soot prediction is strong. For example, Model 9 yields good predictions for seven out of eight flames studied. However, ABF100 would be computationally prohibitive in turbulent flame simulations. Models 8, 16 and 28 give reasonable predictions in six or seven flames out of eight. In fact if the acceptance criterion were extended to a full order of magnitude (0.1–10.0), these models would be shaded for all flames. These models employ acetylene-based nucleation and do not include PAH condensation. This suggests that it may not be necessary to carry gas-phase species up to PAH's.

5. Conclusions

To make progress in soot modeling for luminous turbulent flames, it is important to develop and validate reaction mechanisms/soot models over a broad range of conditions and without the additional complexities of turbulence. Here, seven different ethylene–air mechanisms have been studied to determine their suitability for soot modeling, together with a method of moments for soot particle dynamics. Sensitivity to key soot model parameters has been explored. The assessment has been performed for eight different laminar flames, including both premixed and diffusion flames.

Computed soot volume fractions are most sensitive to variations in surface growth processes (steric factor α, and conserved versus depleted surface radicals). Soot nucleation also influenced soot yields in premixed flames. Acetylene-based (versus PAH-based) nucleation generally performed adequately, and PAH condensation does not appear to be essential. This suggests that relatively small gas-phase reaction mechanisms should suffice. A fruitful line of research for soot modeling would be to develop a function that effectively interpolates between complete depletion and full conservation of surface radicals during the C_2H_2 addition step.

Please cite this article in press as: R.S. Mehta et al., *Proc. Combust. Inst.* (2009), doi:10.1016/j.proci.2008.06.149

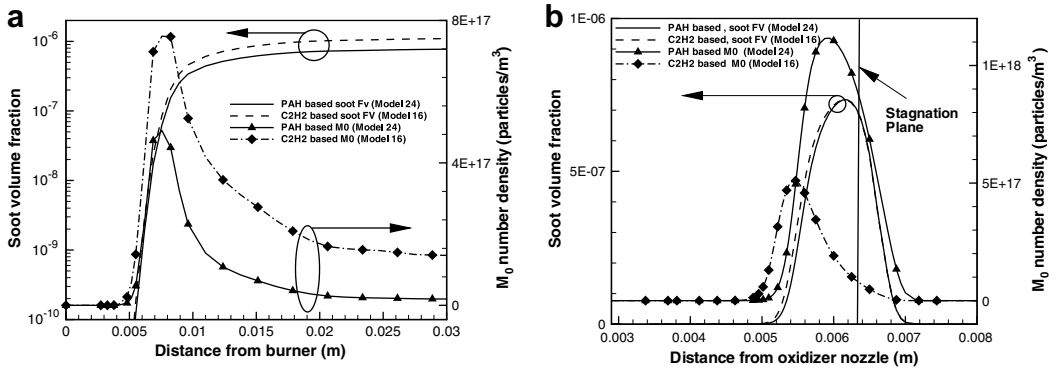

Fig. 5. Effect of nucleation submodels: (a) XSF97_2 premixed flame. (b) WDS96_1 diffusion flame.

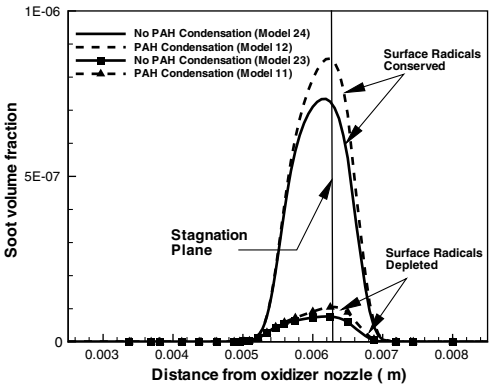

Fig. 6. Effect of PAH condensation: WDS96_1 diffusion flame with and without PAH condensation, with different contributions from surface reactions.

While no model gave soot volume fractions within a factor of five from experimental values for all eight flames, several models are within a factor of 10 for all eight flames. Models 29 and 33 appear promising, for example. Here, oxygen-enriched flames have not been considered. In oxygen-enriched flames, the role of PAH has been found to be higher than in the flames considered here [28]. Soot agglomeration into mass fractals also has not been considered; this is known to be a factor in high-pressure flames [16]. It has been shown that the method of moments has limitations when dealing with bimodal PSDFs (e.g., [28]). The effect of alternative particle dynamics models (e.g., sectional methods) also has not been studied here. Other fuels also are of interest. These extensions are the subjects of ongoing research.

Acknowledgments

This work has been supported by the National Science Foundation under grant #CTS-0121573. The authors thank Dr. Hai Wang (University of Southern California) for discussions about convergence issues in OPPDIF, and Dr. Michael Frenklach (University of California, Berkeley) for help with PREMIX. The first author thanks Dr. Stephen Turns and Kshitij Deshmukh (The Pennsylvania State University) for valuable discussions.

References

[1] I.M. Kennedy, *Prog. Energy Combust. Sci.* 23 (1997) 95–132.
[2] G. Li, M.F. Modest, in: M.P. Mengüç, N. Selçuk (Eds.), *Proceedings of the ICHMT 3rd International Symposium on Radiative Transfer*, Antalya, Turkey, 2001.
[3] R.P. Lindstedt, S.A. Louloudi, *Proc. Combust. Inst.* 30 (2005) 775–783.
[4] B. Zamuner, F. Dupoirieux, *Combust. Sci. Technol.* 158 (2000) 407–438.
[5] M. Frenklach, *Chem. Eng. Sci.* 57 (2002) 2229–2239.
[6] J. Appel, H. Bockhorn, M. Frenklach, *Combust. Flame* 121 (2000) 122–136.
[7] H. Wang, M. Frenklach, *Combust. Flame* 110 (1997) 173–221.
[8] Z. Qin, V.V. Lissianski, H. Yang, W.C. Gardiner, S.G. Davis, H. Wang, *Proc. Combust. Inst.* 28 (2000) 1663–1669.
[9] C.K. Law, *Combust. Sci. Technol.* 177 (2005) 845–870.
[10] Online Resource. URL http://garfield.chem.elte.hu/Combustion/mechmod.htm.
[11] Online Resource. URL http://www-mae.ucsd.edu/combustion/cermech/.
[12] S.C. Li, B. Varatharajan, F.A. Williams, *AIAA paper* 2000-3475.
[13] C.S. McEnally, A.M. Schaffer, M.B. Long, et al., *Proc. Combust. Inst.* 27 (1998) 1497–1505.
[14] M. Frenklach, H. Wang, in: H. Bockhorn (Ed.), *Soot Formation in Combustion: Mechanisms and Models*, Springer-Verlag, New York, 1994.
[15] H. Wang, D.X. Du, C.J. Sung, C.K. Law, *Proc. Combust. Inst.* 26 (1996) 2359–2368.
[16] A. Kazakov, M. Frenklach, *Combust. Flame* 114 (1998) 484–501.

[17] K.M. Leung, R.P. Lindstedt, W.P. Jones, *Combust. Flame* 87 (1991) 289–305.
[18] M. Frenklach, H. Wang, *Proc. Combust. Inst.* 23 (1991) 1559–1566.
[19] S.J. Harris, A.M. Weiner, *Annu. Rev. Phys. Chem.* 36 (1985) 31–52.
[20] K.G. Neoh, J.B. Howard, A.F. Sarofim, in: S.D.C.G. Smith (Ed.), *Particulate Carbon: Formation During Combustion*, Plenum, New York, 1981, p. 261.
[21] M.B. Colket, R.J. Hall, in: H. Bockhorn (Ed.), *Soot Formation in Combustion: Mechanisms and Models*, Springer-Verlag, New York, 1994.
[22] H. Richter, J.B. Howard, *Prog. Energy Combust. Sci.* 26 (2000) 565–608.
[23] R.J. Kee, J.F. Grcar, M. Smooke, J.A. Miller, Tech. Rep. SAND85-8240, Sandia National Laboratories, 1985.
[24] A.E. Lutz, R.J. Kee, J.F. Grcar, F.M. Rupley, Tech. Rep. SAND96-8243, Sandia National Laboratories, 1996.
[25] R.J. Kee, G. Dixon-Lewis, J. Warnatz, M.E. Coltrin, J.A. Miller, Tech. Rep. SAND86-8246, Sandia National Laboratory, 1986.
[26] R.J. Kee, F.M. Rupley, J.A. Miller, Tech. Rep. SAND89-8009B, Sandia National Laboratories, 1989.
[27] F. Xu, P.B. Sunderland, G.M. Faeth, *Combust. Flame* 108 (4) (1997) 471–493.
[28] B. Zhao, Z. Yang, J. Wang, M.V. Johnston, H. Wang, *Aerosol Sci. Technol.* (37) (2003) 611–620.
[29] J. Singh, R.I.A. Patterson, M. Kraft, H. Wang, *Combust. Flame* (145) (2006) 117–127.
[30] J.Y. Hwang, S.H. Chung, *Combust. Flame* 125 (2001) 752–762.

Please cite this article in press as: R.S. Mehta et al., *Proc. Combust. Inst.* (2009), doi:10.1016/j.proci.2008.06.149